EUROPEAN ORGANIZATION FOR NUCLEAR RESEARCH

CERN - SL DIVISION

CERN-SL-2000-057 AP

CLIC Note 446

FINAL-FOCUS SYSTEM FOR CLIC AT 3 TEV

F. Zimmermann, R. Assmann, G. Guignard,

D. Schulte, O. Napoly*

Abstract

We describe a base-line optics for a 3-TeV final-focus system of the Compact Linear Collider (CLIC). The proposed system consists of an initial beta-matching region, two chromatic correction sections, and a final transformer, and it provides a total demagnification by a factor 90 horizontally and 346 vertically. The length per side amounts to 3.3 km. The effect of synchrotron radiation and higher-order aberrations is minimised by an odd dispersion function in the chromatic correction section. For a total flat energy spread of 1%, the system promises a luminosity of about 80% of the ideal. The 20–30% spot-size dilutions in the two transverse planes reflect a trade-off between the Oide effect and higher-order chromo-geometric aberrations.

Paper presented at EPAC2000, 26-30 June 2000, Vienna, Austria

*CEA Saclay

Geneva, Switzerland
08.08.00

FINAL-FOCUS SYSTEM FOR CLIC AT 3 TEV

F. Zimmermann, R. Assmann, G. Guignard, D. Schulte, CERN, Geneva, O. Napoly, CEA/Saclay

Abstract

We describe a base-line optics for a 3-TeV final-focus system of the Compact Linear Collider (CLIC). The proposed system consists of an initial beta-matching region, two chromatic correction sections, and a final transformer, and it provides a total demagnification by a factor 90 horizontally and 346 vertically. The length per side amounts to 3.3 km. The effect of synchrotron radiation and higher-order aberrations is minimised by an odd dispersion function in the chromatic correction section. For a total flat energy spread of 1%, the system promises a luminosity of about 80% of the ideal. The 20–30% spot-size dilutions in the two transverse planes reflect a trade-off between the Oide effect and higher-order chromo-geometric aberrations.

1 INTRODUCTION

The compact linear collider (CLIC) under study at CERN [1] will collide low-emittance electron and positron beams at centre-of-mass energies extending up to 5 TeV. Table 1 compares the design beam parameters at the interaction point (IP) for a 3-TeV CLIC with those actually demonstrated at the SLC and those envisioned for a 1-TeV NLC [2]. The NLC luminosity represents an increase by 4 orders of magnitude compared with the SLC, while the CLIC 3 TeV parameters surpass this by about another factor of ten. The high luminosities are achieved by increasing the number of bunches per rf pulse and, mostly, by reducing the IP spot size. For the latter, one can exploit the natural reduction in geometric emittance at higher energies, but in addition reduced IP beta functions and a significant decrease in the normalised emittances are required.

The task of the final-focus system is to focus the two main beams, after acceleration in the linac, to the transverse design spot sizes of 43 nm, horizontally, and 1 nm, vertically, at the interaction point (IP). The full momentum bandwidth of the final-focus system should be of the order of 1%, in order to accommodate the beam energy spread expected from the linac. The final-focus optics described in this paper nearly fulfills the requirements. The small IP spot size implies tight tolerances on magnet-position and field stability. Both optics calculations and tolerance analyses [3] were performed using the computer codes FFADA [4] and MAD [5].

2 OPTICS

Figure 1 displays the base-line optics for a 3-TeV CLIC final focus. The system consists of a beta-matching region, horizontal and vertical chromatic correction sections (CCX and CCY), and final transformer. The total length is about 3.3 km per side.

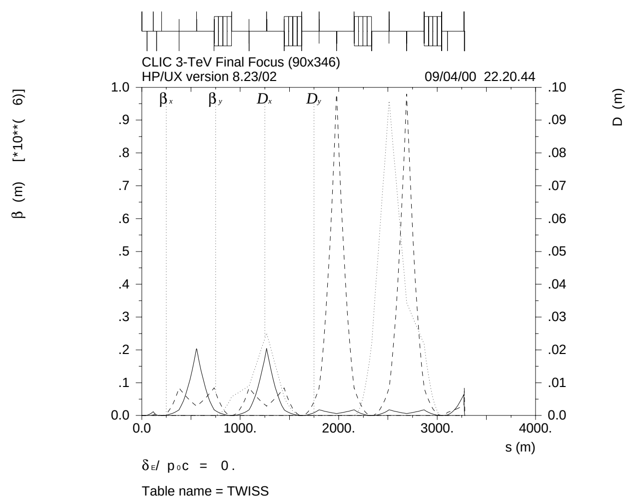

Figure 1: Beta functions and dispersion for the entire final-focus system as a function of the longitudinal position. The interaction point is on the right.

The final focus decreases the initial beam size 90 times and 346 times in the two transverse planes. Most of this

Table 1: IP beam parameters for SLC, NLC and CLIC.

parameter	sym.	SLC	NLC	CLIC
c.m. energy [TeV]	E	0.1	1	3
luminosity [10^{34} cm^{-2} s^{-1}]	L	0.0002	1.3	10
repetition rate [Hz]	f_{rep}	120	120	100
bunch charge [10^{10}]	N_b	3.7	1	0.4
bunches/rf pulse	n_b	1	95	154
bunch spacing [ns]	Δ_b	—	2.8/1.4	0.67
beam power [MW]	P_b	0.04	9	14.8
hor. emittance [μm]	$\gamma\epsilon_x$	50	4.5	0.68
vert. emittance [μm]	$\gamma\epsilon_y$	8	0.1	0.02
hor. beta [mm]	β_x^*	2.8	12	8
vert. beta [mm]	β_y^*	1.5	0.15	0.15
hor. spot size [nm]	σ_x^*	1700†	235	43
vert. spot size [nm]	σ_y^*	900†	4	1.0
bunch length [mm]	σ_z	1	0.12	0.03

† 1998 average value

demagnification occurs in the final transformer, which is made from two quadrupole doublets and which alone demagnifies by a factor 15 horizontally and 50 vertically.

A high gradient of the final quadrupole prior to the IP is necessary in order to confine the doublet chromaticity, which is closely related to the strength of higher-order aberrations. For our base-line design, we have asssumed a quadrupole gradient of 450 T/m. To put this into perspective, an NLC permanent magnet prototype has demonstrated a gradient of 500 T/m [6], and higher values, up to 5000 T/m, are thought to be feasible [7]. For a large aperture s.c. quadrupole the assumed gradient would constitute a 30% increase from present designs [8]. A third possibility is a pulsed quadrupole, which could also achieve gradients of the order of 1000 T/m [9].

We choose a free length from the exit face of the last quadrupole to the IP of 2 m as in the NLC design [2]. With the assumed quadrupole gradients the chromaticity of the final doublet is 6900 in the horizontal and 27000 in the vertical plane. Here, chromaticity is defined in the linear-collider sense as the relative spot-size increase (added in quadrature) divided by the rms energy spread. The beta functions at the entrance to the 5-m long final quadrupole are 15 km horizontally and 88 km vertically, which corresponds to rms beam sizes of 59 μm and 24 μm. This translates into a geometric acceptance of 50–140 σ for a permanent magnet with 3.3-mm bore radius and 450–1100 σ for a superconducting quadrupole with 2.7 cm radial aperture.

The large chromaticity of the final doublet is compensated in the two chromatic correction sections, which feature an odd dispersion function as proposed by Oide [10]. Both chromatic correction sections comprise a pair of sextupoles, separated by a $-I$ transformation and placed an integer multiple of π in betatron phase away from the final doublet. The dispersion is nonzero only at the second sextupole of each pair. This has two advantages: (1) it reduces the number of bending magnets and the amount of synchrotron radiation by a factor of 2, and (2) it avoids many of the 5th-order chromo-geometric aberrations arising from the chromatic breakdown of the $-I$ between the sextupoles, which limit the momentum bandwidth. Thanks to the $-I$ separation the individual sextupole pairs do not generate any 3rd-order geometric aberrations. The 2nd-order dispersion from the CCX is adjusted so as to cancel the 2nd-order dispersion produced in the CCY. The ratio of dispersion values, or, alternatively, the ratio of bending angles in CCX and CCY is thus constrained. In the present design the net bending angles for the dipole regions in CCX and CCY are 63μrad and 230μrad, respectively. The peak beta functions at the CCY sextupoles are about 1000 km, 50 times larger than the peak beta function in the SLC final triplet, and the maximum value of the dispersion is 0.1 m. The initial beta functions of 65 m horizontally and 18 m vertically are chosen equal to the beta functions at the end of the main linac.

In the final transformer the beta functions vary rather dramatically with energy, as is illustrated in Fig. 2. This effect must be taken into account when choosing magnet and beam-pipe apertures.

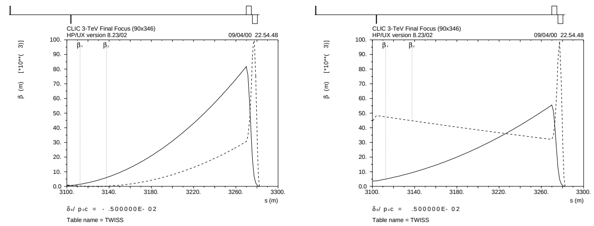

Figure 2: Beta functions in the final telescope for energy offsets of -0.5% [left] and $+0.5\%$ [right].

The system was optimised by varying the total length, the ratio of CCX and CCY lengths, the bending angles, and the strengths of the last two quadrupoles, in order to maximise the luminosity for a 1% flat energy spread. The final parameter choice is a trade-off [11] between Oide effect [12,13] (vertical beam size increase due to synchrotron radiation in the last quadrupoles, favoring a weak second-to-last quadrupole Q2) and the momentum bandwidth in the horizontal plane (demanding a small horizontal chromaticity and, thus, a strong quadrupole Q2).

3 PERFORMANCE

The geometric luminosity, without pinch, is calculated using FFADA by tracking two random sets of particles through the entire system to the interaction point, and convoluting them there on a grid. The luminosity so obtained is displayed in Fig. 3 as a function of the full-width momentum spread assuming a flat energy distribution. For the anticipated energy spread close to 1%, it is about 80% of the ideal value that would be attained for a perfectly linear and achromatic optics, without synchrotron radiation and aberrations.

Figure 4 shows the dependence of the transverse rms spot sizes on the full energy spread $\delta_{\rm FW}$. The vertical spot size is about 30% larger than the ideal value, only slightly increasing with energy spread. The 30% blow-up is due to synchrotron radiation in the second-to-last quadrupole magnet Q2. For small energy spread $\delta_{\rm FW}$ the horizontal spot size is close to the ideal value. However, the latter increases rapidly with increasing $\delta_{\rm FW}$. As indicated above, the strength of Q2 as well as the bending angles in CCX and CCY have been adjusted such that for the nominal 1% energy spread the horizontal blow up is comparable to the vertical.

4 TOLERANCES

Figure 5 displays jitter and drift sensitivities (*i.e.*, the inverse tolerances) for the vertical magnet position. Jitter sensitivities refer to both the induced orbit shift at the IP, which could be corrected over a few pulses, and the IP spot size increase. Drift sensitivies are calculated only from the IP spot-size increase and, thus, they apply over a time interval of several minutes, at which the spot size can be retuned. All numbers in the table correspond to a 2% luminosity loss per magnet. The tightest jitter tolerance is

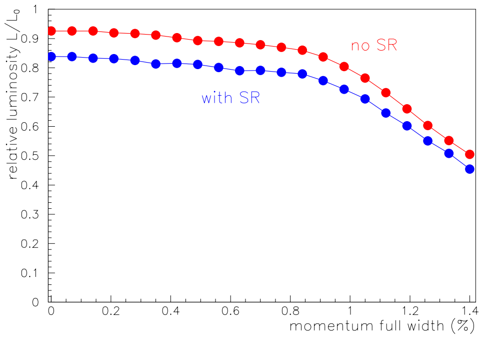

Figure 3: Relative luminosity loss as a function of the full-width energy spread for a flat distribution. The luminosity was calculated by tracking two random distributions of 5000 particles through the final focus to the IP and there convoluting them on a grid. The ideal reference luminosity without pinch is $L_0 = 4.6 \times 10^{34}$ cm^{-2}s^{-1}.

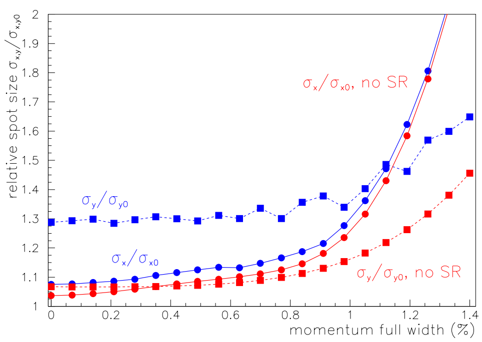

Figure 4: Relative rms spot sizes as a function of the full-width energy spread for a flat distribution with and without synchrotron radiation. The ideal linear spot sizes are $\sigma_{x0} =$ 43 nm and $\sigma_{y0} = 1.0$ nm.

0.2 nm, for the last quadrupole. Various stabilising techniques as well as intra-pulse feedback can be employed to meet this tolerance [14]. Drift tolerances are much looser and of the order of 100 nm. Finally, with sensitivities as shown in Fig. 6, typical field stability tolerances are about 10^{-5}, comparing favorably with the 10^{-6} precision of LHC power converters [15].

5 SUMMARY

We have presented a base-line final focus for 3 TeV. It is 3.3 km long and promises satisfactory performance.

6 REFERENCES

[1] J.P. Delahaye and I. Wilson, "CLIC a multi-TeV e+e- Linear Collider", CERN/PS 99-062 (LP); G. Guignard (ed.), "General Description of a 3 TeV Linear Collider based on the CLIC Technology", in preparation.

[2] C. Adolphsen at el., "NLC Zeroth Order Design Report for the Next Linear Collider", SLAC Report 474 (1996).

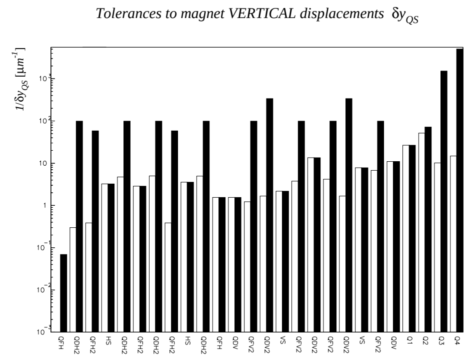

Figure 5: Vertical displacement sensitivity corresponding to a 2% luminosity loss for the various magnets [3, 4]. The full bars represent pulse-to-pulse 'jitter' tolerances, due to both the induced IP orbit motion and IP spot-size increase. The open bars are 'drift' tolerances referring only to increases in the IP beam size.

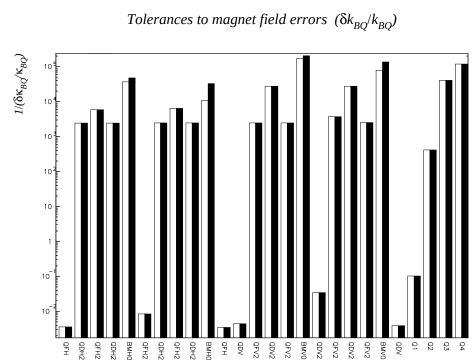

Figure 6: Sensitivities to a relative change in field strength for all final-focus magnets. Again, the full and open bars represent jitter and drift tolerances, respectively.

[3] S. Fartoukh, O. Napoly, EPAC98, Stockholm (2000); S. Fartoukh, Ph.D. thesis, DAPNIA/SEA-97-02T (1997).

[4] O. Napoly and B. Dunham, Proc. EPAC94, London, vol. 1, p. 698 (1994).

[5] H. Grote, F. C. Iselin, CERN-SL-90-13-AP-REV.2 (1990).

[6] J. Spencer, in section 118 of Ref. [2].

[7] K. Egawa and T.M. Taylor, CERN LEP-MA/89-08 and PAC 1989 Chicago (1989).

[8] S. Caspi et al., 15th Int. Conf. Magnet Techn., Bejing (1997).

[9] M. Modena and P. Sievers, CERN/AT-MA/91-24, and Proc. 12th Int. Conf. Magnet Techn., Leningrad (1991).

[10] K. Oide, HEACC'92, Hamburg, p. 2993 (1992).

[11] O. Napoly, CERN-SL-99-054, CLIC Note 414 (1999).

[12] K. Oide, Phys. Rev. Lett. 61, p. 1713 (1988).

[13] K. Hirata, K. Oide, B. Zotter, Phys. Lett. B224, p. 437 (1989).

[14] R. Assmann et al., this conference.

[15] I. Barnett, et al., LHC Project Report 293, PAC 1999.